한국공작기계학회논문집 Vol.17 No.3 2008. 6.
Transactions of the Korean Society of Machine Tool Engineers

Calibration of Acceleration Plant and Test Rig Design to Dynamic Fracture

Jae-Ung Cho*, Moon-Sik Han+

(논문접수일 2007. 11. 8, 심사완료일 2007. 12. 14)

동적 파괴에 대한 가속장치의 보정 및 시험장치 설계

조재웅*, 한문식+

Abstract

The force transducer in the acceleration plant due to dynamic fracture is calibrated by dynamically using the stress pulses from a longitudinal bar. The bar is supported by two strings attached to the ceiling. The bar velocities before and after impact are measured and a full bridge at bar and transducer is formed by the four strain gauges. A transient recorder is used to store the stress pulse signals of force transducer and bar. For the first test series, three point bend test specimens can be chosen by means of test rig design and the inspection as sample experiment in this presented paper is sufficient for proving with the numerical simulation of the specimen model.

Key Words : Acceration plant(가속 장치), Force transducer(힘 변환기), Longitudinal bar(세로 봉), Transient recorder(순간 기록 장치), Stress pulse(응력파), Calibration factor(조정 계수), Three point bend test specimens(삼점 굽힘 시험편들)

1. Introduction

The acceleration plant[1] at Sweden is about 30m long. A sledge runs on two rails. The sledge is pulled by a polyester band which is attached to a piston which runs inside a plastic pipe placed under the rails. The polyester band runs over two rollers at the end of the plant. An air-pressure of the order 1 to 7 bar acts on the piston and the sledge is accelerated. The sledge is at the end of the acceleration plant. The hammer weight is carried on the sledge and 2.4m before hammer impact on the test specimen, the weight is lifted a few mm and then carried on roller bearings. The polyester band used to pull the sledge is between the lead cylinders. The force transducer which is used in the acceleration plant is calibrated dynamically using stress pulses[2,3] from a longitudinal

* 공주대학교 기계·자동차공학부
+ 교신저자, 계명대학교 기계·자동차공학부 (sheffhan@kmu.ac.kr)
주소: 704-701 대구광역시 달서구 신당동 1000번지

bar which hits the force transducer longitudinally. The incoming and outgoing velocities of the bar are measured by means of a speedometer. The momentum transfered to the force transducer is thus determined. The force transducer calibration factor is obtained by dividing the transfered momentum by the integrated force transducer signal. This factor is used to the basic calibration factor in calculating the reaction force due to dynamic fracture. Tests have been made on ordinary 10mm tension test specimens in order to check signal transmission and camera system. The camera available so far is a HIMAC-camara which a maximum capacity of 10,000 frames per second. And the inspection as sample experiment in this presented paper is sufficient for proving with the numerical simulation of the specimen model.

2. Force transducer and test rig design

The force transducer is included in the support, which is attached to two steel plates of 40 and 70mm thickness, see Fig. 1. The steel plates are backed by a $100m^3$ concrete block. A drawing of the force transducer is shown in Fig. 1. Two strain gauges are attached on the upper and lower plane surfaces of the 28mm high tip of the mid support about 20mm from the contact end, see Fig. 1. The force transducer is calibrated for static loading up to 350kN and dynamically by using stress pulses from a 1m long circular bar which hits the transducer longitudinally[4]. Two strain gauges are mounted on each side of the bar(about 25mm from the impact points) in order the detect the time for impact, see Fig. 2. The dilatational stress wave velocity in steel is about 6mm/μs. The first detection at this position is therefore obtained about 4μs after impact. Endevco HBM 3020 C bridge amplifiers are used for the strain gauge channels and the signals were recorded on two NICOLET(2090 and 3091) transient recorders. 1MHz sampling frequency is used.

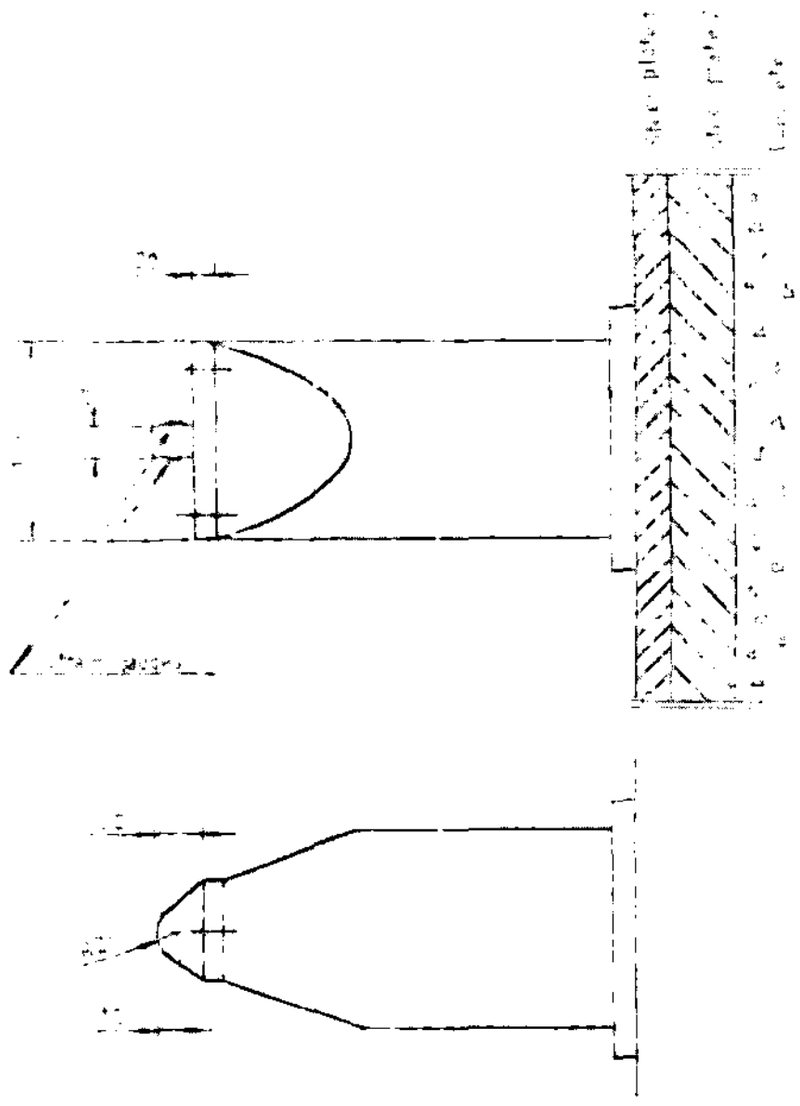

Fig. 1 Force transducer

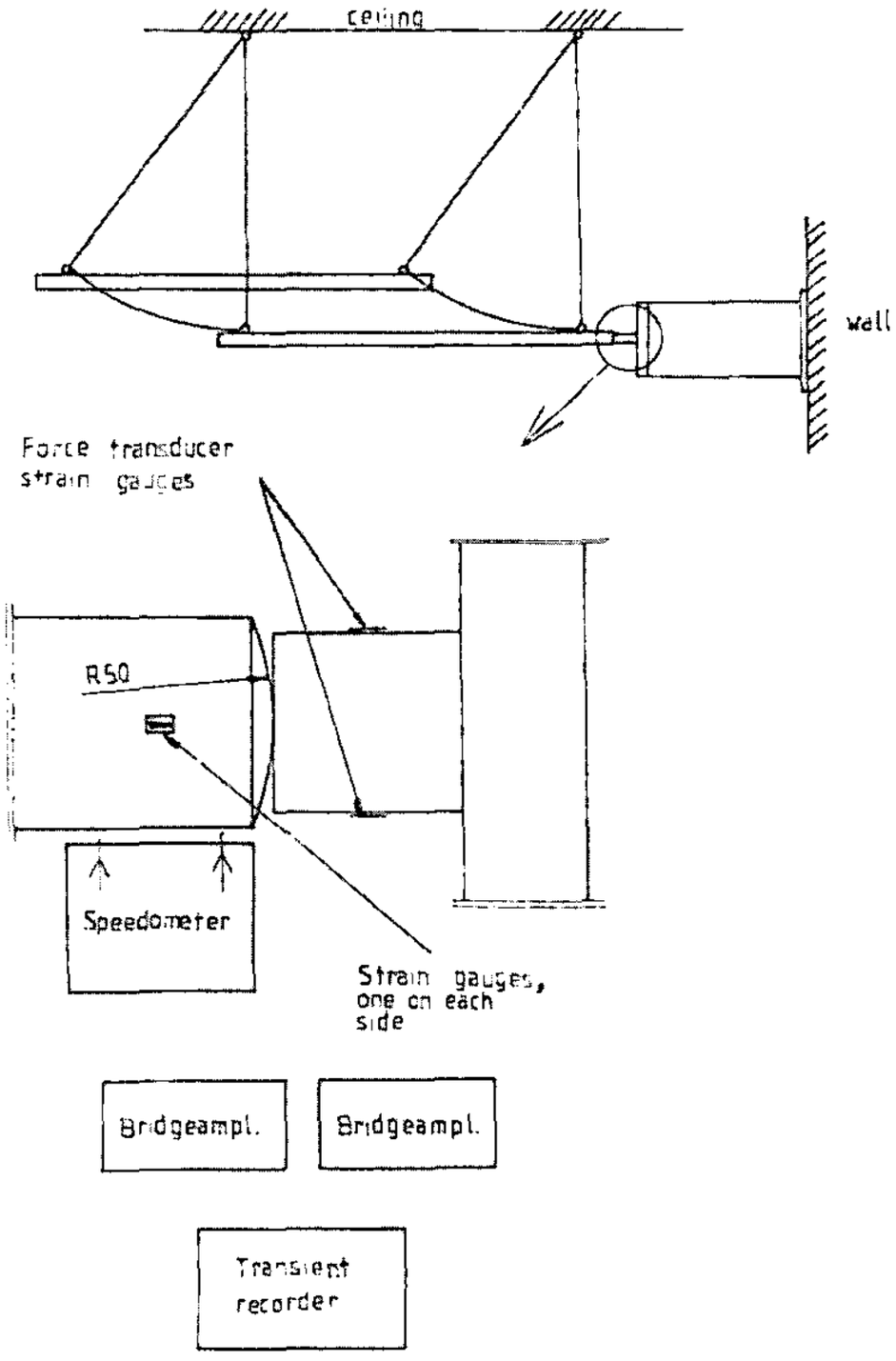

Fig. 2 Calibration system and measurements

One channel on each of the transient recorders is used for the flash-start light detector used in order to calibrate the photos and the electronic recordings. The trigger circuit for the flash and the transient recorder is activated at a hammer position about 5mm in front of the bar. The hammer speed is obtained from the measurement of time to travel 200mm distance.

Fig. 3 shows the layout of the test rig. This figure also shows the successive positions of the specimen when the sledge hammer move to the left. The U-shaped impact head(sledge hammer) hits the rollers attached to the test specimen which is bent over the reaction head. The hammer is arrested through impact on lead cylinders and then bounces to the right. The two parts of the specimen are kept in the frame holders(indicated as two dash-dotted lines) at the end of the test. The test specimen is attached with rollers and carried by two frame holders. Grooves at 10mm spacing are made on the surface. The lead brake cylinders for the hammer are at each side of the reaction head. The lead cylinders have been used twice at a velocity of 14.0m/s and must be replaced and support poles from the sledge brakes are below. Steel shelters are mounted on and below the test area in order to catch parts which may come loose. When hammer weight is at impact position, one of roller bearings for sidewards positioning is up to the right. The mechanical part of the triggering device for the start of registrations from force transducer is in the upper right corner. The strain gauges is placed on the test specimen. For the first test series, three point bend test specimens can be chosen[5,6]. The maximum length of the test specimen, 320mm, is chosen as big as possible with respect to the size of available hammer weights. The length:width:height ratios are chosen as 16:4:1. The length between the rollers are 300mm which give width of 75mm and height of 18.75mm. The first part of the crack is cut in a mill. Crack growth from the V-shaped cut is obtained by fatigue at about 10Hz. High speed photography is used in order to determine the behavior of the crack opening. In order to keep the crack opening area as fixed as possible, a reaction head is placed opposite to the crack. The hammer hits the specimen via two rollers at the ends of the specimen. In this way, minimum motion of the interesting area is obtained and blow-up photos can be taken using a telescope. The specimen is kept close to the reaction head by two frame holders. The two rollers are attached to the

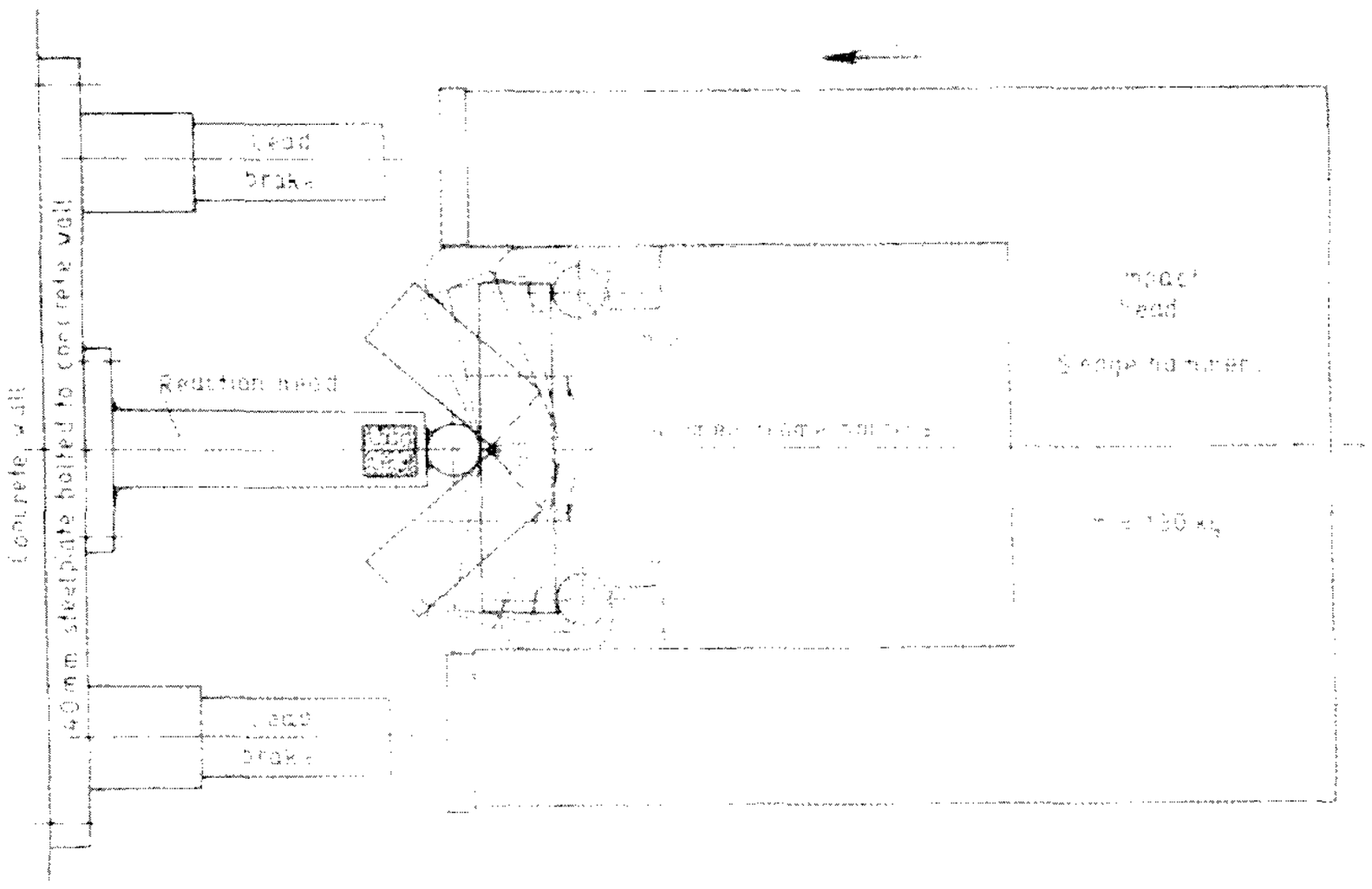

Fig. 3 Layout of the test rig

specimen by means of roller lips. Loose tightened locking screws keep the specimen attached to the frame holders and the rollers attached to the specimen. The forces acting between the locking screws and the test specimen are small and they are judged to influence the mechanical behavior of the system to a vanishingly small degree.

3. Calibration system and calculated results of recorded data

The experimental setup for the calibration system is shown in Fig. 2. The bar is supported by two strings attached to the ceiling. The bar velocities before and after the impact are measured by means of the speedometer. Full bridges in the longitudinal bar and the force transducer are formed by the two active force transducer strain gauges together with two dummy gauges individually. The bridge voltage supply is 5V and the amplification factor is 1000. A transient recorder with sampling frequency 1MHz is used to store the stress pulse signals of force transducer and bar. Fig. 4 and Fig. 5 show the stress pulses in the longitudinal bar and the force transducer signals respectively. Stress pulse signals are shown by multiplying the amplification factor(1000) in output voltage. The calculated results of recorded data are as follows;

◎ Dimensions and the mass of the steel bar:

Diameter : 35.0mm

Length : 1.043m

Mass : 7.827kg

◎ Bar velocities:

V_{in} : 2.15m/s

V_{out} : 1.64m/s

◎ Momentum equation:

$I = M \times (V_{in} + V_{out})$

$= 29.66Ns$(Ns:Newton × Sec)

◎ Integrated force transducer signal:

Integration from 0 to 526μs

$A_{figure} = 4.795 \times 10^{-4}Vs$(Vs:Voltage × Sec)

◎ Calibration factor:

$\alpha = I \div A_{figure}$

$= 61900N/V$(N/V:Newton/V)

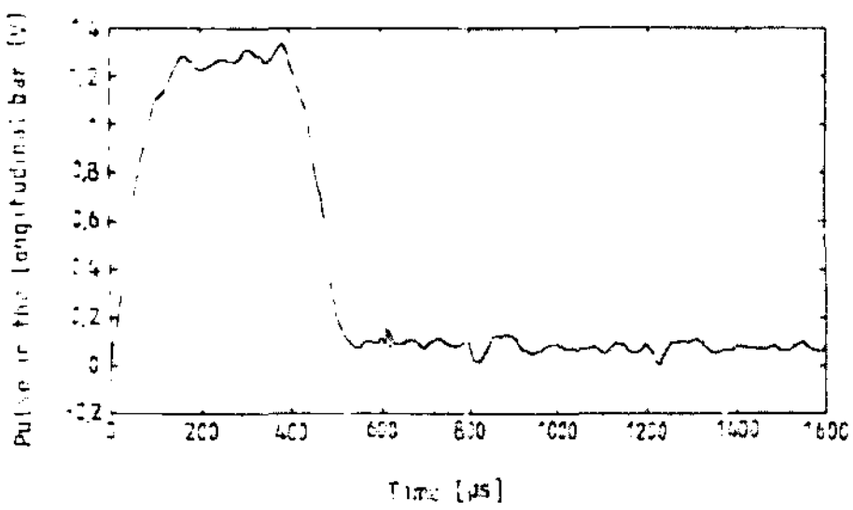

Fig. 4 Stress pulse in the longitudinal bar

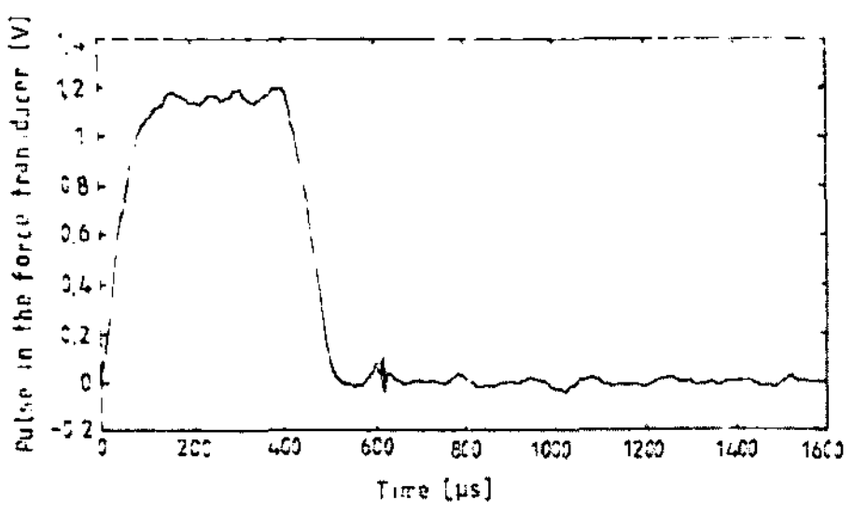

Fig. 5 Stress pulse in the force transducer

4. Inspection as the sample experiment

The geometry of the specimen and the finite element model are shown in Fig. 6 and Fig. 7. These dimension parameters are given as shown in Fig. 6 as follows.

Due to the symmetry, only half a specimen is modeled. A two-dimensional mesh including 92 eight node plane stress elements with 2*2 Gauss points, i. e. with reduced integration, is chosen. The mesh near the crack tip is

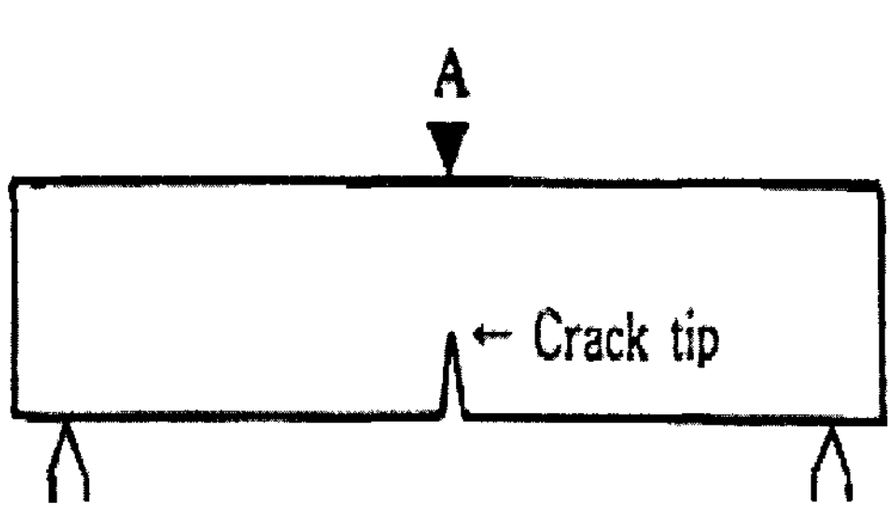

Fig. 6 Geometry of the specimen

concentrated by using the degenerated eight node elements. In order to model a possible loss of contact at the load point A and at the support points B which had been discussed[7], gap elements with one degree of freedom are introduced. Furthermore, a lumped mass element is used to model the impact head as shown in Fig. 7. No crack propagation is taken into account in the calculations. The dynamical J-integral and CMOD are calculated using the commercial finite element method code, ABAQUS[8]. In this code, the virtual crack extension method is successfully used to evaluate the J-integral in the dynamic case[9,10].

The experiment is run at impact velocity of 45m/s to inspect this simulation model in this study. The dynamically loaded 3-point bending(3PB) ductile steel specimens are made to compare with numerical simulation. The geometry of this specimen is same to Fig. 7. This material is Mn-alloyed normalized steel. The result of tensile test is shown in Fig. 8. The experimental display was also explained at Fig. 6.

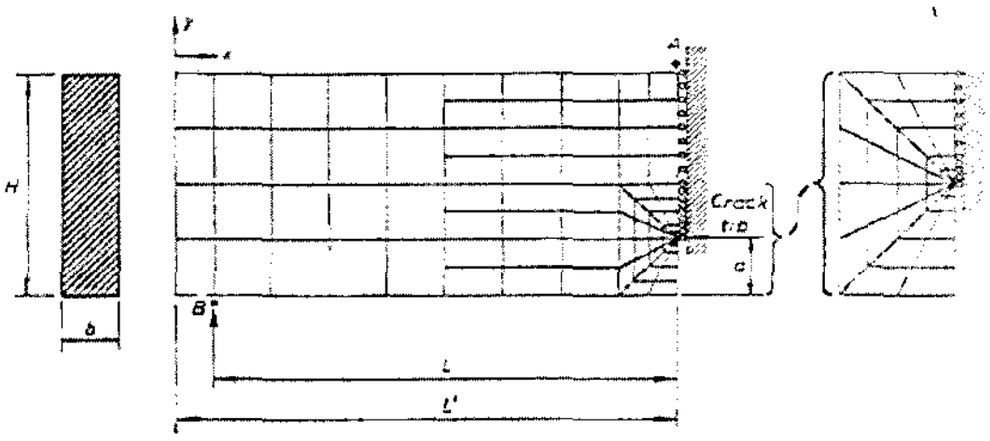

Fig. 7 Finite element model for 3PB specimen with a quarter notch(L=300mm, L′=320mm, H=75mm, b=18mm, a=H/4=18.75mm)

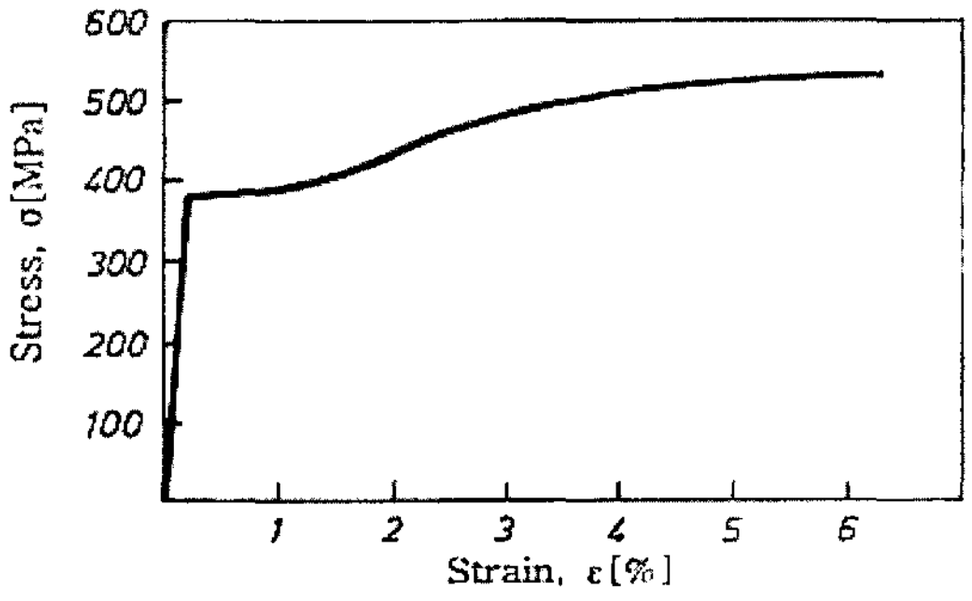

Fig. 8 Static tensile test diagram

The U-shaped hammer is accelerated to a prescribed velocity and hits the 3PB specimen at the side points B as shown in Fig. 6. This specimen is supported at the middle point A. Two hardened and tempered impact heads with cylindrical contact surfaces are attached to the hammer. The recordings during the experiments include high speed photography, mid support force measurements and impact detection. Plane stress in FEM simulation is made under the assumption of no crack growth. The material of this specimen is treated as an elastic-plastic material using an isotropic hardening von Mises model, i.e., the possible effects of rate dependent material properties are ignored. The used mesh is same to Fig. 7 in this study. The side points B of the specimen are impacted by a U-shaped hammer. Due to the bending of the specimen, the friction forces parallel with the specimen surface may be introduced during impact. To investigate this aspect, two different boundary conditions at the impact points are considered in the simulations: roller and locking. The mid support forces obtained from the experiments and the simulations are presented in Fig. 9 for the impact velocity of 45m/s. It is notable that the experiments give the results which become closer to the numerical simulation with the locking boundary condition than with the roller boundary condition. The CMOD

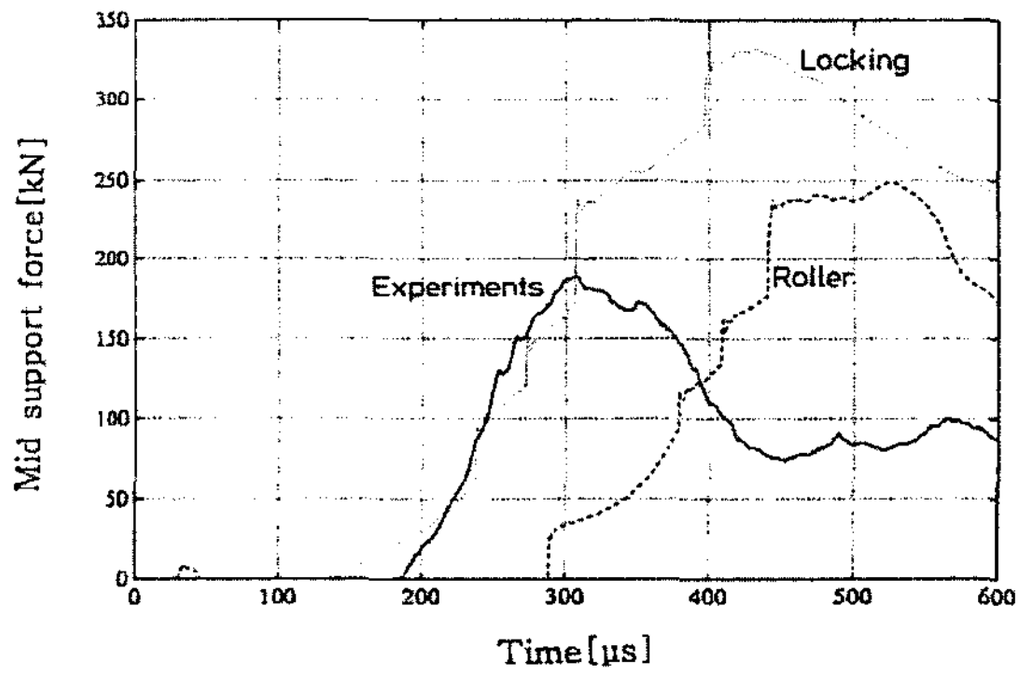

Fig. 9 Mid-support force versus time at the impact velocity of 45m/s for the two different simulations and the experiment(experiment: solid line, simulations, roller boundary: broken line, locking boundary: dotted line)

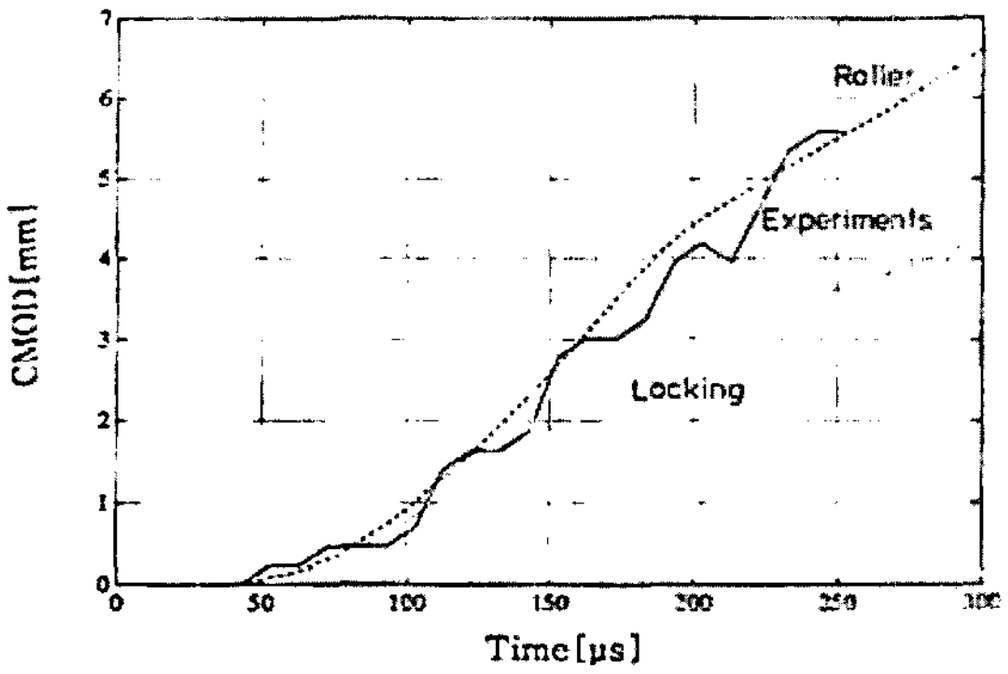

Fig. 10 CMOD versus time at the impact velocity of 45m/s for the two different simulations and the experiment(experiment: solid line, simulations, roller boundary: broken line, locking boundary: dotted line)

simulations for both sets of the boundary conditions are also shown in Fig. 10 for the impact velocity of 45m/s together with the experimentally found values. The experiments for CMOD curves become closer to the numerical simulation with locking boundary condition than with the roller boundary condition as shown in Fig. 9. Therefore, the inspection as sample experiment in this presented paper is sufficient for proving with the numerical simulation of the specimen model.

5. Conclusions

The result can be summarized as follows.

(1) Calibration system in the dynamic acceleration plant can be set up experementally.
(2) The force transducer calibration factor can be obtained by dividing the transfered momentum by the integrated force transducer signal.
(3) Calibration factor of force transducer at the acceleration plant is 61900N/V in this study.
(4) Calibration factor found in this study can be used as the basic calibration factor in calculating the reaction force due to dynamic fracture.
(5) For the first test series, three point bend test specimens can be chosen by means of test rig design and the inspection as sample experiment in this presented paper is sufficient for proving with the numerical simulation of the specimen model.

References

(1) Wihlborg, G., 1985, "Design and Application of a Rig for High Energy Impact Tests," *IUTAM Symposium*, Tokyo/Japan.
(2) Kolsky, H., 2003, *Stress Waves in Solids*, Dover Publication Inc., New York.
(3) Li-li, W., 2007, *Foundations of Stress Waves*, Elsevier Science Ltd., England.
(4) Bergmark, A. and Cho, J. U., 1991, "Dynamic Calibration of Force Transducer," *Sweden Technical Report LUTFD2/(TFHF-3046)*, pp. 1~5.
(5) HAN, M. S., Bergmark, A. and Cho, J. U., 2005, "STUDY ON DYNAMIC BEHAVIOUR IN 3PB DUCTILE STEEL SPECIMEN APPLIED BY THE IMPACT LOAD," *International Journal of Automotive Technology*, Vol. 6, No.3, pp. 229~234.
(6) HAN, M. S. and Cho, J. U., 2006, "CORRELATION BETWEEN J-INTEGRAL AND CMOD IN IMPACT BEHAVIOR OF 3-POINT BEND SPECIMEN," *International Journal of Automotive Technology*, Vol. 7, No. 3, pp. 337~344.
(7) Bergmark, A. and Kao, H. R., 1991, "Dynamic crack initiation in 3PB ductile steel specimens," *Technical Report, LUTFD2 TFHF-3041, Lund Institute of Technology*, Sweden, pp. 1~23.
(8) Hibbitt, D., 1989, *ABAQUS Manual: Version 4.8*, Karlsson and Sorensen Inc., USA.
(9) Nakamura, T., Shin, C. F., and Freund, L. B., 1985, "Elastic-Plastic Analysis of a Dynamically Loaded Circumferentially Notched Round Bar," *Eng. Frac. Mech.*, No. 22, pp. 437~452.
(10) Cho, J. U. and Han, M. S., 2007, "Study on the Dynamic Fracture of Rod Impacting on Plate at High Speed," *Transactions of the Korean Society of Machine Tool Engineers*, Vol. 16, No. 4, pp. 108~112.